

# 3D Quantum Trajectories. Quantum orbits of the Hydrogen's electron

T. Djama\*

November 20, 2018

## Abstract

In this paper, we introduced the 3D-Quantum Stationary Hamilton Jacobi Equation for a central potential, and established the 3D quantum law of motion of an electron in the presence of such a potential. We established a system of three differential equations from which, and as a numerical application, we plotted the 3D quantum trajectories of the Hydrogen's electron for the ground state and two excited states. we did a comparison between a supposed classical trajectory of the hydrogen electron and the corresponding QTs. We found out that for a particular set of the hidden variables, the QT is close in its shape to the classical one.

PACS: 03.65.Bz; 03.65.Ca

Key words: three dimension, quantum law of motion, atomic potential, quantum trajectories.

---

\*Electronic address: [djamatoufik@yahoo.fr](mailto:djamatoufik@yahoo.fr)

## 1. Introduction

More than five years ago, we presented a deterministic approach of quantum mechanics in 3D [1] based on the 3D Quantum Stationary Hamilton Jacobi Equation (3D-QSHJE)

$$\frac{1}{2m_0} \left( \vec{\nabla} S_0(\vec{r}) \right)^2 - \frac{\hbar^2}{2m_0} \frac{\Delta A(\vec{r})}{A(\vec{r})} + (E - V(\vec{r})) = 0 \quad , \quad (1)$$

$$\vec{\nabla} \cdot \left( A^2(\vec{r}) \vec{\nabla} S_0 \right) = 0 \quad . \quad (2)$$

In that work, we established the solution of the 3D-QSHJE to be of the form

$$S_0(\vec{r}) = \hbar \arctan \left( \frac{\Psi_1(\vec{r})}{\Psi_2(\vec{r})} \right) \quad , \quad (3)$$

where  $\Psi_1$  and  $\Psi_2$  are two real independent solutions of the 3D Schrödinger equation (SE). The expression of the function  $A(\vec{r})$  is given as

$$A(\vec{r}) = \sqrt{\Psi_1^2 + \Psi_2^2} \quad . \quad (4)$$

In addition, we established the 3D quantum law of motion [1]

$$\vec{v} \cdot \vec{\nabla} S_0 = 2 [E - V(\vec{r})] \quad . \quad (5)$$

This last equation is the one that should be used to plot the 3D quantum trajectories (QTs).

The establishment of the 3D quantum law of motion (Eq. (5)) for a general form of the potential is an important step to investigate the 3D motions. However, we should plot the 3D QTs when it is possible in order to understand the behavior of the quantum particle's motion in 3D spaces. With this aim, we should proceed exactly as we have done for the 1D quantum and relativistic QTs [2, 3]. Indeed, we must first solve the 3D SE to find the functions  $\Psi_1$  and  $\Psi_2$ , which we take into the expression of the reduced action (Eq. 3). Then, we take expression (3) into Eq. (5). After solving Eq. (5), we can plot the QTs. Note that for a general potential, plotting the 3D QTs is not obvious due to the complexity of the problem. This is why, in this article, we study the case of the central potential, and plot the trajectories of an electron moving under the atomic potential.

The paper is organized as follows: In Sec. 2, we introduce the 3D-QSHJE and its solutions for the central potential. Then, in Sec. 3, we rewrite the quantum law of motion for this potential and establish a system of three differential equations that describe the dynamical behavior of the quantum particles. After that, in Sec. 4, we plot the classical trajectories of a particle moving under the action of the atomic potential. In Sec. 5, we plot the 3D QTs of the Hydrogens electron for several bound states. Finally, In Sec. 6, we present a conclusion in which we discuss our results.

## 2. The 3D-QSHJE for the central potential

In order to construct the 3D-QSHJE in the case of a central potential, we write the 3D SE with respect to the spherical coordinates  $(r, \vartheta, \varphi)$  [4]

$$\frac{\partial^2 \Psi}{\partial r^2} + \frac{2}{r} \frac{\partial \Psi}{\partial r} + \frac{1}{r^2} \frac{\partial^2 \Psi}{\partial \vartheta^2} + \frac{\cot \vartheta}{r^2} \frac{\partial \Psi}{\partial \vartheta} + \frac{1}{r^2 \sin^2 \vartheta} \frac{\partial^2 \Psi}{\partial \varphi^2} + \frac{2m_0}{\hbar^2} [E - V(r)] \Psi = 0 \quad , \quad (6)$$

$\Psi(r, \vartheta, \varphi)$  is the wave function of the considered quantum system. To solve Eq. (6), the variables must be separated into  $\Psi(r, \vartheta, \varphi)$  as [4]

$$\Psi(r, \vartheta, \varphi) = R(r)T(\vartheta)F(\varphi) ,$$

where  $R(r)$  is the radial wave function,  $T(\vartheta)$  and  $F(\varphi)$  are the angular wave functions. It follows that Eq. (6) will be separated into three equations, each one corresponds to one variable,

$$\frac{r^2}{R} \frac{d^2 R}{dr^2} + \frac{2r}{R} \frac{dR}{dr} + \frac{2m_0 r^2}{\hbar^2} (E - V(r)) = l(l+1) , \quad (7)$$

$$\frac{d^2 T}{d\vartheta^2} + \cot \vartheta \frac{dT}{d\vartheta} + \left( l(l+1) - \frac{m_l^2}{\sin^2 \vartheta} \right) T = 0 , \quad (8)$$

$$\frac{d^2 F}{d\varphi^2} + m_l^2 F = 0 . \quad (9)$$

$l$  being a positive integer or nil, and  $m_l$  is an integer satisfying to

$$-l \leq m_l \leq l .$$

$l(l+1)$  is the eigen value of  $L^2$ ,  $L$  representing the angular momentum operator.  $m_l$  represents the eigen value of  $L_z$ , the operator projection of  $L$  along the  $z$  axis. Now, let us write Eqs. (7), (8) and (9) in a form analogous to the 1D SE. First, we take up Eq. (7) and write

$$R(r) = \frac{\mathcal{X}(r)}{r} , \quad (10)$$

where  $\mathcal{X}(r)$  is a function of the radius. This will allow us to write

$$\frac{-\hbar^2}{2m_0} \frac{d^2 \mathcal{X}}{dr^2} + \left[ V(r) + \frac{\lambda \hbar^2}{2m_0 r^2} \right] \mathcal{X} = E \mathcal{X} . \quad (11)$$

This last equation has the same form as the 1D SE with a fictitious potential

$$V'(r) = V(r) + \frac{\lambda \hbar^2}{2m_0 r^2} . \quad (12)$$

Likewise, Eq. (8) can be reduced to the form of the 1D SE by introducing the function

$$\mathcal{T}(\vartheta) = \sin^{\frac{1}{2}} \vartheta T(\vartheta) \quad (13)$$

into Eq. (8), we will find

$$\frac{d^2 \mathcal{T}}{d\vartheta^2} + \left( \lambda + \frac{1}{4} \right) \mathcal{T} + \frac{(1/4 - m_l^2)}{\sin^2 \vartheta} \mathcal{T} = 0 . \quad (14)$$

Remark that Eq. (14) has the form of the 1D SE with a fictitious potential

$$V(\vartheta) = \frac{\hbar^2}{2m_0} \frac{(m_l^2 - 1/4)}{\sin^2 \vartheta} , \quad (15)$$

and an energy

$$E_\vartheta = \left( \lambda + \frac{1}{4} \right) \frac{\hbar^2}{2m_0} . \quad (16)$$

Remark also that Eq. (9) has the same form as the 1D SE with a vanishing potential and an energy equal to  $m_l^2 \hbar^2 / 2m$ . Because Eqs. (7), (8) and (9) come to the form of the 1D SE, in order to obtain three separated 1D-QSHJEs, let us write the functions  $\mathcal{A}(r)$ ,  $\mathcal{T}(\vartheta)$  and  $F(\varphi)$  as

$$\Psi(r, \vartheta, \varphi) = \mathcal{A}(r)\xi(\vartheta)\eta(\varphi) \left[ \alpha e^{\frac{i}{\hbar}[Z(r)+L(\vartheta)+M(\varphi)]} + \beta e^{-\frac{i}{\hbar}[Z(r)+L(\vartheta)+M(\varphi)]} \right], \quad (17)$$

where  $\mathcal{A}(r)\xi(\vartheta)\eta(\varphi) = A(r, \vartheta, \varphi)$  is the amplitude of the wave function, and  $S_0(r, \vartheta, \varphi) = Z(r) + L(\vartheta) + M(\varphi)$  is the total reduced action. (Expressing the total reduced action as a sum of three 1D reduced actions is argued in Ref. [5] in the case of cartesian symmetry potentials. For the case of the central potential, the separation of the variables in the reduced action still valid and one can prove it by proceeding by the same way as in Ref. [5]. By replacing Eq. (17) in Eqs. (7), (8) and (9) respectively, we obtain exactly as we had proceeded in 1D

$$\frac{1}{2m_0} \left( \frac{dZ}{dr} \right)^2 - \frac{\hbar^2}{4m_0} \{Z, r\} + V(r) + \frac{l(l+1)\hbar^2}{2m_0 r^2} = E, \quad (18)$$

$$\left( \frac{dL}{d\vartheta} \right)^2 - \frac{\hbar^2}{2} \{L, \vartheta\} + \frac{(m_l^2 - 1/4)\hbar^2}{\sin^2 \vartheta} = \left( l(l+1) + \frac{1}{4} \right) \hbar^2, \quad (19)$$

$$\left( \frac{dM}{d\varphi} \right)^2 - \frac{\hbar^2}{2} \{M, \varphi\} = m_l^2 \hbar^2. \quad (20)$$

Eqs. (18), (19) and (20) represent the components of the QSHJE in 3-D for a central potential. These equations contain the Schwarzian derivatives of the functions  $Z$ ,  $L$  and  $M$  with respect to  $r$ ,  $\vartheta$  and  $\varphi$  respectively. Note that, by deducing the value of  $\lambda$  from Eq. (18), and the value of  $m_l$  from Eq. (20), then substituting it in Eq. (19), one obtains

$$\frac{1}{2m_0} \left( \vec{\nabla}_{r, \vartheta, \varphi} S_0 \right)^2 - \frac{\hbar^2}{4m_0} \left[ \{S_0, r\} + \frac{1}{r^2} \{S_0, \vartheta\} + \frac{1}{r^2 \sin^2 \vartheta} \{S_0, \varphi\} \right] + V(r) - \frac{\hbar^2}{8m_0 r^2} - \frac{\hbar^2}{8m_0 r^2 \sin^2 \vartheta} = E. \quad (21)$$

Eq. (21) represents the QSHJE in 3-D for a central potential. At the classical limit ( $\hbar \rightarrow 0$ ), Eq. (21) goes to the Classical Stationary Hamilton-Jacobi Equation (CSHJE). Remark that taking the classical limit in Eqs. (18), (19) and (20) makes  $dL/d\vartheta$  and  $dM/d\varphi$  vanish, then, one cannot obtain the CSHJE. We deduce that the classical limit must be taken into Eq. (21). Note also that separating variables in Eq. (21), we get to Eqs. (18), (19) and (20) which lead to Eqs. (7), (8) and (9). After separating variables in Eq. (21), three constants of motion appear, they are the energy  $E$ ,  $l(l+1)$  and  $m_l$ .

The solutions of Eqs. (18), (19) and (20) are respectively

$$Z(r) = \hbar \arctan \left\{ \alpha_r \frac{\mathcal{X}_2}{\mathcal{X}_1} + b_r \right\} = \hbar \arctan \left\{ a_r \int \frac{dr}{\mathcal{X}_1^2} + b_r \right\}, \quad (22)$$

$$L(\vartheta) = \hbar \arctan \left\{ \alpha_\vartheta \frac{\mathcal{T}_2}{\mathcal{T}_1} + b_\vartheta \right\} = \hbar \arctan \left\{ a_\vartheta \int \frac{d\vartheta}{\mathcal{T}_1^2} + b_\vartheta \right\}, \quad (23)$$

$$M(\varphi) = \hbar \arctan \left\{ \alpha_\varphi \frac{F_2}{F_1} + b_\varphi \right\} = \hbar \arctan \left\{ a_\varphi \int \frac{d\varphi}{F_1^2} + b_\varphi \right\}, \quad (24)$$

where  $\alpha_r, b_r, \alpha_\vartheta, b_\vartheta, \alpha_\varphi, b_\varphi, a_r, a_\vartheta$  and  $a_\varphi$  are real constants.  $\mathcal{X}_1$  and  $\mathcal{X}_2$  are two real independent solutions of Eq. (11).  $\mathcal{T}_1$  and  $\mathcal{T}_2$  are two real independent solutions of Eq. (14).  $F_1$  and  $F_2$  are two real independent solutions of Eq. (9).

Before introducing the quantum law of motion, we would like to remind the fact that for the central potential, only the radial function  $\mathcal{X}$  depends on the form of the potential, meaning that the two angular functions  $\mathcal{T}$  and  $F$  can be established without considering the form of the central potential. Indeed, if we take a look on the table of solutions of the SE for such a potential we should write the angular function  $\mathcal{T}_1$  as [6]

$$\mathcal{T}_1^{(l m_l)}(\vartheta) = (1 - \cos^2(\vartheta))^{\frac{|m_l|}{2} + \frac{1}{4}} \frac{d^{l+|m_l|}}{d(\cos(\vartheta))^{l+|m_l|}} [(1 - \cos^2(\vartheta))^l], \quad (25)$$

and the angular function  $F_1$  as

$$\begin{aligned} F_1(\varphi) &= \sin(|m_l|\varphi) & \text{if } m_l \neq 0 \\ &= 1 & \text{if } m_l = 0, \end{aligned} \quad (26)$$

up to normalization constants.

### 3. The Quantum law of motion for a particle moving under the central potential

Now let us investigate the quantum law of motion for the central potential case. Knowing that the 3D quantum law of motion is given by Eq. (5) and using the spherical coordinates in it, we may write

$$\dot{r} \frac{dZ}{dr} + \dot{\vartheta} \frac{dL}{d\vartheta} + \dot{\varphi} \frac{dM}{d\varphi} = 2[E - V(r)]. \quad (27)$$

As in classic mechanics, we do not use directly Eq. (27) to plot the trajectories. We must first, separate the variables  $r, \vartheta$  and  $\varphi$ . This seems not possible from Eq. (27), and must be done in the 3D QSHJE (Eq. (21)). We noted in Sec. 2 that the separation of variables in Eq. (21) leads directly to Eqs. (18), (19) and (20). In Ref. [1], we have considered a deformation of the space like for general relativity. This idea was based on the quantum coordinate introduced in a earlier work of Faraggi and Matone [7]. We treated the 3D quantum systems with a general potential by using the mechanics of a deformed space. This allowed us to introduce a quantum Lagrangian and derive the quantum law of motion (Eq. (5)). For the central potential, we proceed with the same manner. Thus, let us write Eq. (21) as

$$\begin{aligned} \left( \frac{dZ}{dr} \right)^2 g_{rr}(r) + \frac{1}{r^2} \left( \frac{dL}{d\vartheta} \right)^2 g_{\vartheta\vartheta}(\vartheta) + \\ \frac{1}{r^2 \sin^2(\vartheta)} \left( \frac{dM}{d\varphi} \right)^2 g_{\varphi\varphi}(\varphi) = 2m_0[E - V(r)], \end{aligned} \quad (28)$$

where

$$g_{rr}(r) = 1 - \frac{\hbar^2}{2} \left( \frac{dZ}{dr} \right)^{-2} \{Z, r\},$$

$$g_{\vartheta\vartheta}(\vartheta) = 1 - \frac{\hbar^2}{2} \left( \frac{dL}{d\vartheta} \right)^{-2} \left( \{L, \vartheta\} - \frac{1}{2} \right), \quad (29)$$

and

$$g_{\varphi\varphi}(\varphi) = 1 - \frac{\hbar^2}{2} \left( \frac{dM}{d\varphi} \right)^{-2} \left( \{M, \varphi\} - \frac{1}{2} \right),$$

are real functions depending on  $r$ ,  $\vartheta$  and  $\varphi$  respectively. They represent the non-vanishing components of the metric tensor of the curved space created by the central potential. Now, if one identifies the energy  $E$  to the quantum hamiltonian  $H$ , and using the canonical equations  $\partial H/\partial P_r = \dot{r}$ ,  $\partial H/\partial P_\vartheta = \dot{\vartheta}$  and  $\partial H/\partial P_\varphi = \dot{\varphi}$  he gets

$$\frac{dZ}{dr} = m_0 \dot{r} g_{rr}, \quad (30)$$

$$\frac{dL}{d\vartheta} = m_0 r^2 \dot{\vartheta} g_{\vartheta\vartheta}, \quad (31)$$

$$\frac{dM}{d\varphi} = m_0 r^2 \sin^2(\vartheta) \dot{\varphi} g_{\varphi\varphi}. \quad (32)$$

Taking expressions of  $g_{rr}$ ,  $g_{\vartheta\vartheta}$  and  $g_{\varphi\varphi}$  from the last three equations and replacing them into Eq. (28), we deduce Eq. (27), while replacing them into Eqs. (18), (19) and (20) respectively after taking into account of relations (29), we find

$$\frac{dZ}{dr} \dot{r} = 2 \left[ E - V(r) - \frac{l(l+1)\hbar^2}{2m_0 r^2} \right], \quad (33)$$

$$\frac{dL}{d\vartheta} \dot{\vartheta} = \frac{l(l+1)\hbar^2}{m_0 r^2} - \frac{(m_l^2 - 1/4)\hbar^2}{m_0 r^2 \sin^2(\vartheta)}, \quad (34)$$

$$\frac{dM}{d\varphi} \dot{\varphi} = \frac{(m_l^2 - 1/4)\hbar^2}{m_0 r^2 \sin^2(\vartheta)}. \quad (35)$$

The three above relations represent the decomposition of Eq. (27) with respect to the variables  $r$ ,  $\vartheta$  and  $\varphi$ . Indeed, if one takes the sum of Eqs. (33), (34) and (35) he finds Eq. (27). In fact, these equations describe the dynamical behaviour of a particle moving under the central potential, each one describes it in the corresponding coordinate ( $r$ ,  $\vartheta$  or  $\varphi$ ). Note that only Eq. (33) depends on the nature of the central potential  $V(r)$  while Eqs. (34) and (35) do not depend on it. However, they depend implicitly on the radial potential via the radial position  $r$ .

As an application of the 3D quantum law of motion (Eqs. (27), (33), (34) and (35)), we propose in the following sections to plot the trajectories of an electron moving under the action of the Hydrogen potential (Hydrogen atom). This will allow us to acquire more comprehension of the 3D quantum law of motion.

#### 4. Classical trajectories of a particle moving under a central potential

Before plotting the QTs, it will be useful to present the classical Hamilton-Jacobi formulation of mechanics and also to plot the classical trajectory of a particle moving under the central potential. The Hamilton-Jacobi formulation

is based on the CHJE. In the case of a central potential, the separation of the variables in the CHJE gives

$$\left(\frac{dZ}{dr}\right)^2 = 2m_0 \left[ E - V(r) - \frac{\alpha}{2m_0 r^2} \right], \quad (36)$$

$$\left(\frac{dL}{d\vartheta}\right)^2 = \alpha - \frac{\beta^2}{\sin^2(\vartheta)}, \quad (37)$$

and

$$\left(\frac{dM}{d\varphi}\right)^2 = \beta^2. \quad (38)$$

$\alpha$  and  $\beta$  are real constants. As we know, the momenta  $dZ/dr$ ,  $dL/d\vartheta$  and  $dM/d\varphi$  are connected to the speeds  $\dot{r}$ ,  $\dot{\vartheta}$  and  $\dot{\varphi}$  as follows

$$\frac{dZ}{dr} = m_0 \dot{r}, \quad (39)$$

$$\frac{dL}{d\vartheta} = m_0 r^2 \dot{\vartheta}, \quad (40)$$

$$\frac{dM}{d\varphi} = m_0 r^2 \sin^2(\vartheta) \dot{\varphi}. \quad (41)$$

Taking these last equations into Eqs. (36), (37) and (38), we find

$$\dot{r} = \pm \sqrt{\frac{2}{m_0}} \sqrt{E - V(r) - \frac{\alpha}{2m_0 r^2}}, \quad (42)$$

$$\dot{\vartheta} = \pm \frac{1}{m_0 r^2} \sqrt{\alpha - \frac{\beta^2}{\sin^2(\vartheta)}}, \quad (43)$$

$$\dot{\varphi} = \pm \frac{\beta}{m_0 r^2 \sin^2(\vartheta)}, \quad (44)$$

The  $\pm$  signs in Eqs. (42), (43) and (44) indicate that the motion of the particle may be in either direction on the  $r$  axis,  $\vartheta$  circle and  $\varphi$  semicircle respectively. Now, we can integrate Eqs. (42), (43) and (44) to deduce the three time equation with respect to the coordinates  $r$ ,  $\vartheta$  and  $\varphi$ , but before, we write these equations as

$$\sqrt{\frac{2}{m_0}} dt = \pm \frac{dr}{\sqrt{E - V(r) - \alpha/(2m_0 r^2)}}, \quad (45)$$

$$\frac{dt}{m_0 r^2} = \pm \frac{d\vartheta}{\sqrt{\alpha - \beta^2/\sin^2(\vartheta)}}, \quad (46)$$

$$\frac{dt}{m_0 r^2 \sin^2(\vartheta)} = \pm \frac{d\varphi}{\beta}. \quad (47)$$

We remark that Eq. (45) can be integrated directly after knowing the form of the central potential (either analytically or numerically). However, to integrate Eq. (46), we must first write  $r$  -already integrated from Eq. (45)- in function of  $t$ . Also, to integrate Eq. (47), we should set the variables  $r$  and  $\vartheta$  in function of

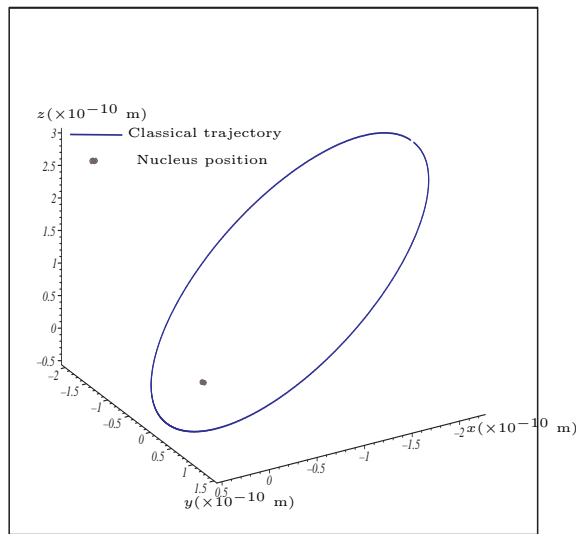


Fig1. Classical 3D trajectory of the Hydrogen's electron. In order to consider the atomic scalars, we have chosen in Eqs (71-73),  $E = -13.6/4$  eV,  $\alpha = 2\hbar^2$  and  $\beta = (\sqrt{3}/2)\hbar^2$ . It is an ellipse, and we see clearly that the motion is done in a plan.

$t$ . In spite of the importance of the time equations, we will focus on the spatial trajectory equations. These last's can be derived directly from Eqs. (45), (46) and (47) after parameterizing the time  $t$ . Thus, we deduce

$$\sin^2(\vartheta)d\varphi = \pm \frac{\beta dr}{r^2 \sqrt{2m_0(E - V(r)) - \alpha/r^2}}, \quad (48)$$

$$\frac{d\vartheta}{\sqrt{\alpha - \beta^2/\sin^2(\vartheta)}} = \pm \frac{dr}{r^2 \sqrt{2m_0(E - V(r)) - \alpha/r^2}}, \quad (49)$$

$$d\varphi = \pm \frac{d\vartheta}{\sin(\vartheta)\sqrt{(\alpha/\beta^2)\sin^2(\vartheta) - 1}}. \quad (50)$$

Integrating these last equations we find the trajectory equation  $\mathcal{F}(r, \vartheta, \varphi) = 0$ . In order to compare the classical trajectories with the QTs, we plot in Fig.1 the trajectory of an electron under the atomic potential (Hydrogen atom)

$$V(r) = -\frac{k e^2}{r}, \quad (51)$$

where  $k = 9.10^9 S.I$  is the electric constant and  $e$  the charge of the electron. We give the energy  $E$  the value  $-(13.6/4)$  eV, which corresponds in the quantum case to the energy of the first excited state ( $n = 2$ ,  $n$  being the principle number). This is in order to compare the classical trajectory (Fig.1) with the QTs corresponding to this value of energy. For the same reason, we have chosen the constants  $\alpha = 2\hbar^2$  and  $\beta = (\sqrt{3}/2)\hbar$  equal to the values of  $l(l+1)\hbar^2$  and  $\sqrt{m_l^2 - 1/4}\hbar$  respectively, for  $l = 1$  and  $m_l = 1$ . Then, the QTs corresponding to the classical trajectory are those plotted for  $n = 2$ ,  $l = 1$  and  $m_l = 1$  (Figs.7 and 8).



The classical trajectory shown in Fig.1 is an inclined ellipse. This trajectory is obviously famous since it is analogous to the trajectory of a planet submitted to the gravitation force of the sun.

## 5. Quantum orbits of the Hydrogen's electron

In this section we will plot the 3D QTs. First, let us rewrite Eqs. (33), (34) and (35) as follows

$$2 dt = \left[ E - V(r) - \frac{l(l+1)\hbar^2}{2m_0r^2} \right]^{-1} \frac{dZ}{dr} dr, \quad (52)$$

$$dt = \frac{m_0r^2}{\hbar^2} \left[ l(l+1) - \frac{(m_l^2 - 1/4)}{\sin^2(\vartheta)} \right]^{-1} \frac{dL}{d\vartheta} d\vartheta, \quad (53)$$

$$dt = \frac{m_0r^2 \sin^2(\vartheta)}{(m_l^2 - 1/4)\hbar^2} \frac{dM}{d\varphi} d\varphi. \quad (54)$$

By integrating Eqs. (52), (53) and (54) we find the time equations. In order to plot the QTs, we need to find the trajectories equations. In this order, we parameterize the time  $dt$  into Eqs. (52), (53) and (54) so as to obtain

$$\frac{\sin^2(\vartheta)}{(m_l^2 - 1/4)} \frac{dM}{d\varphi} d\varphi = \left[ \frac{2m_0}{\hbar^2} r^2 (E - V(r)) - l(l+1) \right]^{-1} \frac{dZ}{dr} dr, \quad (55)$$

$$\left[ l(l+1) - \frac{(m_l^2 - 1/4)}{\sin^2(\vartheta)} \right]^{-1} \frac{dL}{d\vartheta} d\vartheta = \left[ \frac{2m_0}{\hbar^2} r^2 (E - V(r)) - l(l+1) \right]^{-1} \frac{dZ}{dr} dr, \quad (56)$$

$$\frac{dM}{d\varphi} d\varphi = \left[ \frac{l(l+1)}{(m_l^2 - 1/4)} \sin^2(\vartheta) - 1 \right]^{-1} \frac{dL}{d\vartheta} d\vartheta. \quad (57)$$

In what follows Eqs. (55), (56) and (57) are used to plot the 3D quantum spatial trajectories (orbits). Expressions of the quantum momenta  $dZ/dr$ ,  $dL/d\vartheta$  and  $dM/d\varphi$  are deduced directly from the corresponding quantum reduced actions  $Z$ ,  $L$  and  $M$  (Eqs. (22), (23) and (24) respectively)

$$\frac{dZ}{dr} = \pm \frac{\hbar a_r \mathcal{X}_1^{-2}}{\left( a_r \int \frac{dr}{\mathcal{X}_1^2} + b_r \right)^2 + 1}, \quad (58)$$

$$\frac{dL}{d\vartheta} = \pm \frac{\hbar a_\vartheta \mathcal{T}_1^{-2}}{\left( a_\vartheta \int \frac{d\vartheta}{\mathcal{T}_1^2} + b_\vartheta \right)^2 + 1}, \quad (59)$$

$$\frac{dM}{d\varphi} = \pm \frac{\hbar a_\varphi F_1^{-2}}{\left( a_\varphi \int \frac{d\varphi}{F_1^2} + b_\varphi \right)^2 + 1}. \quad (60)$$

Knowing the expressions of the functions  $\mathcal{X}_1$ ,  $\mathcal{T}_1$  and  $F_1$ , the system of the three differential equations (55-57) can be solved numerically for the different values

of the constants  $a_r$ ,  $b_r$ ,  $a_\vartheta$ ,  $b_\vartheta$ ,  $a_\varphi$  and  $b_\varphi$ . The  $\pm$  sign in the expressions of the quantum momenta shows the fact that the motion of the particle may be in either direction of the  $r$  axis,  $\vartheta$  semicircle and  $\varphi$  circle.

**Note:** In fact two of Eqs. (55), (56) and (57) are sufficient to integrate and determine the quantum spatial trajectories since the third equation is automatically satisfied when the two others are.

Now, let us consider the quantum motion of the Hydrogen's electron. We take up the expression of the atomic potential given in Eq. (51). In this case, the solving of Eq. (11) is obvious and gives for the radial function  $\mathcal{X}$  the following expression [6]

$$\mathcal{X}_1^{(nl)}(r) = \exp\left(\frac{r}{na_o}\right) \left(\frac{r}{a_o}\right)^{-l} \frac{d^{n-l-1}}{dr^{n-l-1}} \left[ \left(\frac{r}{a_o}\right)^{n+l} \exp\left(-\frac{2r}{na_o}\right) \right] \quad (61)$$

$n$  being an integer number representing the principle quantum number, and

$$a_o = \frac{\hbar^2}{m_0 k e^2}$$

is the Bohr's radius. The function  $\mathcal{X}_1^{(nl)}$  corresponds to the energy

$$E_n = -\frac{k e^2}{2 n^2 a_o}.$$

Fixing the values of  $n$ ,  $l$  and  $m_l$  into Eqs. (61), (25) and (26) and substituting these equations into Eqs. (58), (59) and (60) respectively, then replacing these lasts' into Eqs. (55-57) after taking account of the above expressions of the Bohr's radius and the energy, we get a system of three differential equations which after integrating leads to the 3D QTs of the electron for the corresponding bound state  $(n, l, m_l)$ . Naturally, these trajectories depend on the constants  $a_r$ ,  $b_r$ ,  $a_\vartheta$ ,  $b_\vartheta$ ,  $a_\varphi$  and  $b_\varphi$ . So, for several sets of those constants it corresponds many trajectories (See Figs. (2-7)). In other words, for each bound state many trajectories exist exactly as we have found for the 1D quantum motions. This shows the existence of microstates that the QSHJE detects and that are not detected by the SE as it is shown in 1D in Ref. [8]. We will show this by plotting the trajectories of three bound states, the fundamental state ( $n = 1$ ,  $l = 0$ ,  $m_l = 0$ ), and the excited bound states ( $n = 2$ ,  $l = 0$ ,  $m_l = 0$ ) and ( $n = 2$ ,  $l = 1$ ,  $m_l = 1$ )<sup>1</sup>. With this aim, for each state we proceed as follows:

First, we explicit the functions  $\mathcal{X}_1^{(nl)}$ ,  $\mathcal{T}_1^{(lm)}$  and  $F_1^{(m_l)}$  from Eqs. (61), (25) and (26). Secondly, we integrate numerically Eq. (52) and plot the time equation  $r(t)$  for different values of the constants  $a_r$  and  $b_r$ . After, by numerical methods we integrate the two Eqs. (55) and (57) for different values of the constants by setting  $\varphi$  as the free variable varying from  $-\pi$  to  $\pi$  or multiple values of this angle. Then, we plot the resulted data to show the quantum spatial trajectories.

---

<sup>1</sup>The considered excited states in this article do not obeys to the selection law that we consider in spectroscopy of the Hydrogen atom. We just use these states in order to make a simple description of the QTs for different values of the quantum numbers  $n$ ,  $l$  and  $m_l$ .

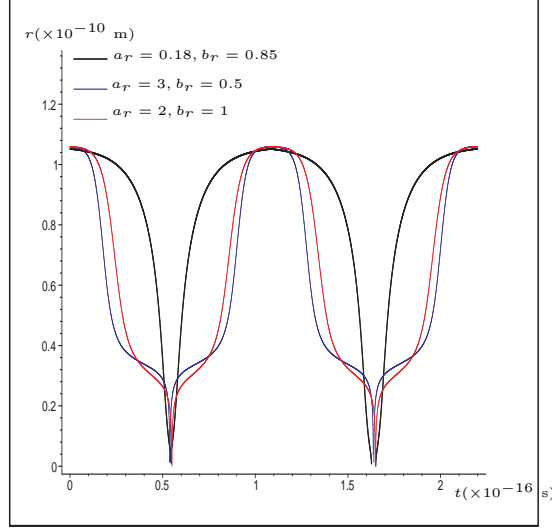


Fig2. Quantum radial time trajectories for the Hydrogen's electron in the fundamental state ( $E = -13.6$  eV,  $n = 1$ ,  $l = 0$ ,  $m_l = 0$ ). For all the curves, we have chosen  $r(t = 0) = 2a_o$  ( $a_o = 0.52917 \cdot 10^{-10}$  m is the Bohr radius).

### a- the fundamental state

For this state, we have  $n = 1$ ,  $l = 0$  and  $m_l = 0$ . The functions  $\mathcal{X}_1^{(10)}$ ,  $\mathcal{T}_1^{(00)}$  and  $F_1^{(0)}$  are deduced from Eqs. (61), (25) and (26) as

$$\mathcal{X}_1^{(10)}(r) = \frac{r}{a_o} \exp\left(-\frac{r}{a_o}\right), \quad (62)$$

$$\mathcal{T}_1^{(00)}(\vartheta) = \sin^{\frac{1}{2}}(\vartheta), \quad (63)$$

$$F_1^{(0)}(\varphi) = 1. \quad (64)$$

Replacing Eqs. (62), (63) and (64) into Eqs. (58), (59) and (60), we find

$$\frac{dZ}{dr} = \pm \frac{\hbar a_r \left(\frac{r}{a_o}\right)^{-2} e^{\frac{2r}{a_o}}}{(a_r I_1(r) + b_r)^2 + 1}, \quad (65)$$

$$\frac{dL}{d\vartheta} = \pm \frac{\hbar a_\vartheta \sin^{-1}(\vartheta)}{[a_\vartheta \log(|\tan(\frac{\vartheta}{2})|) + b_\vartheta]^2 + 1}, \quad (66)$$

$$\frac{dM}{d\varphi} = \pm \frac{\hbar a_\varphi}{(a_\varphi \varphi + b_\varphi)^2 + 1}, \quad (67)$$

where

$$I_1(r) = \int \left(\frac{a_o}{r}\right)^2 \exp\left(\frac{2r}{a_o}\right) dr = -\frac{a_o^2}{r} \exp\left(\frac{2r}{a_o}\right) - 2a_o \text{Ei}\left(1, -2\frac{r}{a_o}\right),$$

Ei being the exponential integral function. We should notice here that we are interested only on the real part of the function Ei and not on the imaginary part, in fact, we should write  $\Re(\text{Ei})$ . Replacing Eq. (65) into Eq. (52), we find

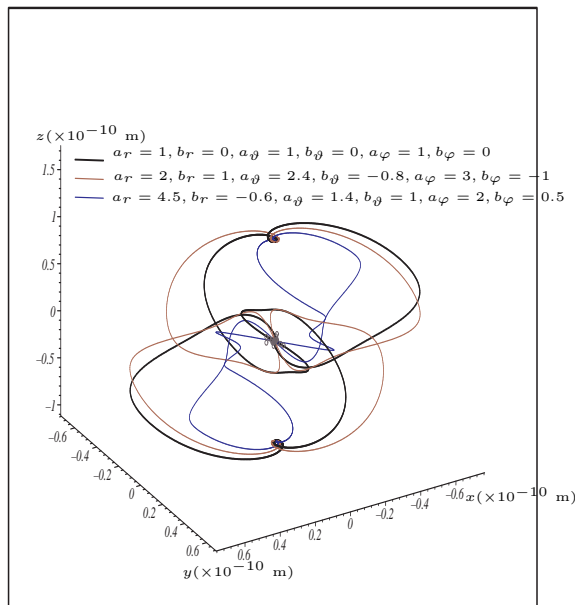


Fig3. Quantum 3D spatial trajectories of the Hydrogen's electron in the fundamental state ( $E = -13.6$  eV,  $n = 1$ ,  $l = 0$ ,  $m_l = 0$ ).

$$\frac{\hbar}{m_0} dt = \pm \left( -\frac{r^2}{a_o^2} + \frac{2r}{a_o} \right)^{-1} \left[ \frac{a_r a_o^2 e^{\frac{2r}{a_o}}}{(a_r I_1(r) + b_r)^2 + 1} \right] dr, \quad (68)$$

which after integrating numerically, we plot the radial time trajectories given in Fig.2. In this figure, the electron moves between two radial extremities  $r = 0$  and  $r = 2a_o$ , and describes different trajectories for the same state. All these trajectories pass through some points constituting nodes with the same manner as for the 1D motions [2, 3]. The radial position  $r = 0$  of the nodes correspond to the zero of the radial function  $\mathcal{X}_1^{(10)}$ . In particular, the nodes situated at  $r = 2a_o$  correspond to the vanishing value of the radial velocity given by Eq. (68). It appears that the radial velocities at  $r = 0$  take not vanishing values<sup>2</sup> meaning that, in the space, the electron when it reaches  $r = 0$  continues its spatial trajectory to reach the  $r = 2a_o$  in the opposite side of the previous position  $r = 2a_o$ . When the electron reaches this extremity  $r = 2a_o$ , its velocity vanishes and turns back to the position  $r = 0$  from which it will continue to the other extremity  $r = 2a_o$ . This makes the number of extremities  $r = 2a_o$  two and the number of the spatial trajectory's cut branches four (Fig.3). Remark that all the trajectories oscillate about the trajectory for which the radial hidden variables take the values  $a_r = 0.18$  and  $b_r = 0.85$ . Now, taking Eqs. (65), (66)

<sup>2</sup> In fact, if one computes the limit of the radial velocities at  $r = 0$  from Eq. (68), he will find  $\infty$ . This infinite velocities appears in our equations for this case and the next case because we did not consider relativistic effects yet. We think that for the quantum relativistic theory corresponding to our approach we will avoid these infinite velocities.

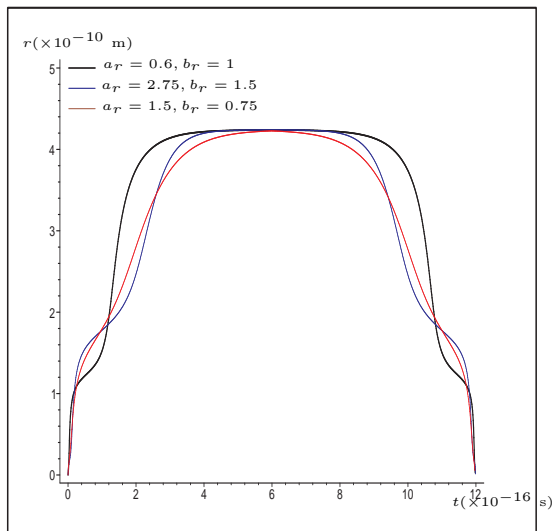


Fig4. Quantum radial time trajectories for the Hydrogen's electron in the first excited state ( $E = -13.6/4$  eV,  $n = 2, l = 0, m_l = 0$ ). For all the curves, we have chosen  $r(t = 0) = 0$ .

and (67) into Eqs. (55) and (57), we get

$$\frac{4 a_\varphi \sin^2(\vartheta)}{(a_\varphi \varphi + b_\varphi)^2 + 1} d\varphi = \pm \frac{a_r a_o^2 \left(-\frac{r^2}{a_o^2} + \frac{2r}{a_o}\right)^{-1} r^{-2} e^{\frac{2r}{a_o}}}{(a_r I_1(r) + b_r)^2 + 1} dr, \quad (69)$$

$$\frac{a_\varphi}{(a_\varphi \varphi + b_\varphi)^2 + 1} d\varphi = \pm \frac{a_\vartheta \sin^{-1}(\vartheta)}{[a_\vartheta \log(|\tan(\frac{\vartheta}{2})|) + b_\vartheta]^2 + 1} d\vartheta. \quad (70)$$

Integrating the last two equations, we plot the 3D quantum spatial trajectories given in Fig.3. This figure shows that the Hydrogen's electron traces different trajectories which all pass from the position  $r = 0$  and the two extremities  $r = 2a_o$ , these three positions constitute nodes for the trajectories. The position  $r = 0$  can be seen as the position of the nucleus in a first approximation and we may deduce that the electron fall on the nucleus. This is not the case because both electron and nucleus make a relative motion compared to their gravity center, so that the nucleus oscillate between the two radial positions  $r_{nuc} = 0$  and  $r_{nuc}^{max} = \frac{m_o}{m_o + M_{nuc}} r_{el}^{max}$ , (for the hydrogen  $r_{nuc} \simeq 10^{-13} \times m$ ). Then the electron has a real possibility to pass through the position  $r_{el} = 0$  without collision with the nucleus. It is useful to indicate that the motion of the electron in a state for which  $m_l = 0$  is a purely quantum motion and cannot have a classical correspondent. The reason is because in Eqs. (37) and (38),  $\beta^2$  can never take negative values while in Eq. (34) and (35),  $(m_l^2 - 1/4)\hbar^2$  takes a negative value for  $m_l = 0$ .

**b- excited state:  $n = 2, l = 0, m_l = 0$**

For this state, the radial function  $\mathcal{X}_1^{(20)}$  is

$$\mathcal{X}_1^{(20)}(r) = \left(\frac{r}{a_o}\right) \left(2 - \frac{r}{a_o}\right) \exp\left(-\frac{r}{2a_o}\right), \quad (71)$$

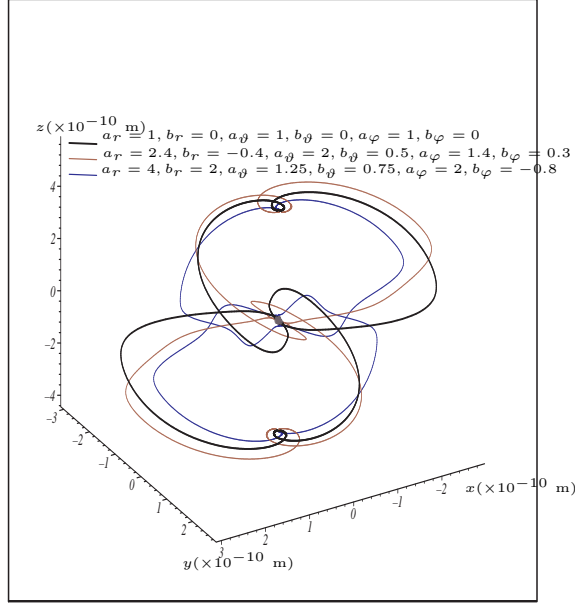


Fig5. Quantum 3D spatial trajectories of the Hydrogen's electron in the first excited state ( $E = -13.6/4$  eV,  $n = 2$ ,  $l = 0$ ,  $m_l = 0$ ).

while the angular functions still given by Eqs. (63) and (64). Replacing Eq. (71) into Eq. (58), we find

$$\frac{dZ}{dr} = \pm \frac{\hbar a_r \left(\frac{r}{a_o}\right)^{-2} \left(2 - \frac{r}{a_o}\right)^{-2} e^{\frac{r}{a_o}}}{(a_r I_2(r) + b_r)^2 + 1}, \quad (72)$$

where

$$\begin{aligned} I_2(r) &= \int \left(\frac{a_o}{r}\right)^2 \left(2 - \frac{r}{a_o}\right)^{-2} \exp\left(\frac{r}{a_o}\right) dr \\ &= -\frac{a_o}{4} \frac{\exp\left(\frac{r}{a_o}\right)}{\frac{r}{a_o} - 2} - \frac{1}{4} \frac{a_o^2}{r} \exp\left(\frac{r}{a_o}\right) - \frac{a_o}{2} \text{Ei}\left(1, -\frac{r}{a_o}\right), \end{aligned}$$

Taking Eq. (72) into Eq. (52), we find

$$\frac{\hbar}{m_0} dt = \pm \left(-\frac{r^2}{4a_o^2} + \frac{2r}{a_o}\right)^{-1} \left[ \frac{a_r a_o^2 \left(2 - \frac{r}{a_o}\right)^{-2} e^{\frac{r}{a_o}}}{(a_r I_2(r) + b_r)^2 + 1} \right] dr, \quad (73)$$

Integrating numerically Eq. (73), we plot the radial time equation for this bound state (Fig.4). In this figure, the electron moves between two radial positions  $r = 0$  and  $r = 8a_o$  through different trajectories. All these trajectories pass through some nodes. The radial positions  $r = 0$  of the nodes correspond to the zeros of the radial function  $\mathcal{X}_1^{(20)}$ . In particular, the nodes situated at  $r = 8a_o$  correspond to the vanishing value of the radial velocity given by Eq. (73). The

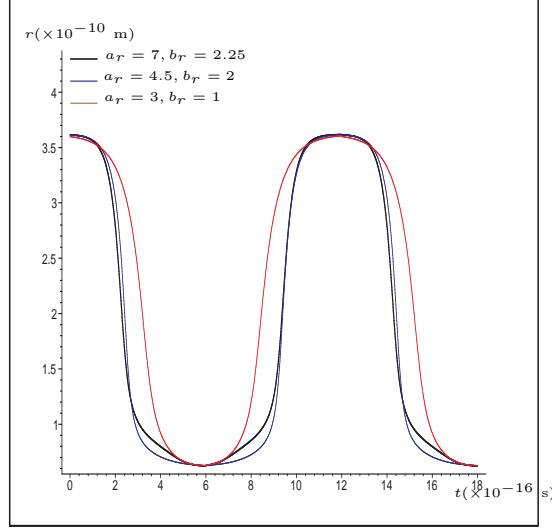


Fig6. Quantum radial time trajectories for the Hydrogen's electron in the second excited state ( $E = -13.6/4$  eV,  $n = 2, l = 1, m_l = 1$ ). For all the curves, we have chosen  $r(t = 0) = 0$ .

radial velocities do not vanish at  $r = 0$  making the electron going through this position toward another extremity  $r = 8a_0$  different from the previous one in the same way as for the ground state case. Thus, there are two extremities  $r = 8a_0$  and four trajectories cut branches ( $r_{extr1} = 8a_0 \rightarrow r = 0$ ;  $r = 0 \rightarrow r_{extr2} = 8a_0$ ;  $r_{extr2} = 8a_0 \rightarrow r = 0$  and  $r = 0 \rightarrow r_{extr2} = 8a_0$ ).

Taking Eqs. (72), (66) and (67) into Eqs. (55) and (57), we get

$$\frac{4 a_\varphi \sin^2(\vartheta)}{(a_\varphi \varphi + b_\varphi)^2 + 1} d\varphi = \pm \frac{a_r a_o^2 \left( -\frac{r^2}{4a_o^2} + \frac{2r}{a_o} \right)^{-1} \left( 2 - \frac{r}{a_o} \right)^{-2} r^{-2} e^{\frac{r}{a_o}}}{(a_r I_2(r) + b_r)^2 + 1} dr, \quad (74)$$

and Eq. (70). Integrating Eqs. (74) and (70) we plot the 3D quantum spatial trajectories given in Fig.5 for this state. This figure shows clearly that for different values of the hidden variables the electron traces different trajectories that all pass from three nodes situated at  $r = 0$  and the two extremities  $r = 8a_0$ .

### c- excited state: $n = 2, l = 1, m_l = 1$

For this state, the radial function is

$$\mathcal{X}_1^{(21)}(r) = \left( \frac{r}{a_o} \right)^2 \exp \left( -\frac{r}{2a_o} \right), \quad (75)$$

and the angular functions are

$$\mathcal{T}_1^{(11)}(\vartheta) = \sin^{\frac{3}{2}}(\vartheta), \quad (76)$$

$$F_1^{(1)} = \sin(\varphi), \quad (77)$$

without taking into account of the multiplicative constant  $(-2)$  obtained in the calculation of  $\mathcal{T}_1^{(11)}$ . Replacing Eqs. (75), 76 and (77) into Eqs. (58), (59) and (60), we find

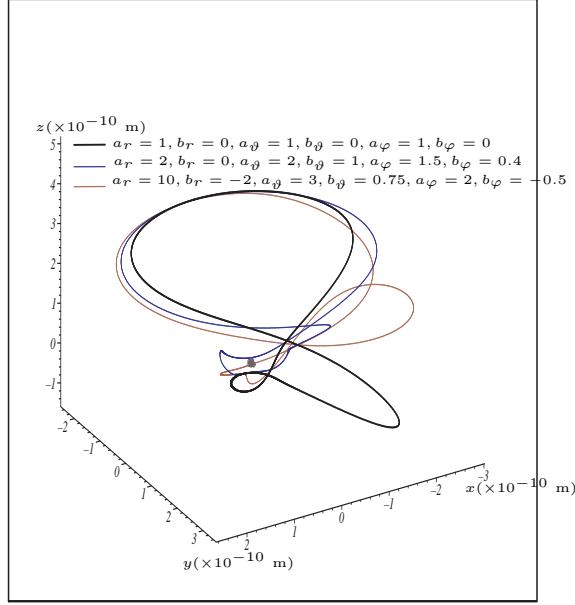


Fig7. Quantum 3D spatial trajectories of the Hydrogen's electron in the third excited state ( $E = -13.6/4$  eV,  $n = 2$ ,  $l = 1, m_l = 1$ ).

$$\frac{dZ}{dr} = \pm \frac{\hbar a_r \left(\frac{r}{a_o}\right)^{-4} e^{\frac{r}{a_o}}}{(a_r I_3(r) + b_r)^2 + 1}, \quad (78)$$

$$\frac{dL}{d\vartheta} = \pm \frac{\hbar a_\vartheta \sin^{-3}(\vartheta)}{\left[ a_\vartheta \left( \frac{\cos(\vartheta)}{\cos(2\vartheta)-1} + \frac{1}{2} \log(|\tan(\frac{\vartheta}{2})|) \right) + b_\vartheta \right]^2 + 1}, \quad (79)$$

$$\frac{dM}{d\varphi} = \pm \frac{\hbar a_\varphi}{(a_\varphi \sin(\varphi) + b_\varphi \cos(\varphi))^2 + \cos(\varphi)^2}, \quad (80)$$

where

$$\begin{aligned} I_3(r) &= \int \left(\frac{r}{a_o}\right)^{-4} \exp\left(\frac{r}{a_o}\right) dr \\ &= -\frac{a_o}{3} \left[ \frac{a_o}{r} \exp\left(\frac{r}{a_o}\right) \left[ \left(\frac{a_o}{r}\right)^2 + \frac{1}{2} \frac{a_o}{r} + \frac{1}{2} \right] + \frac{1}{2} \text{Ei}\left(1, -\frac{r}{a_o}\right) \right]. \end{aligned}$$

Taking Eq. (78) into Eqs. (52), we find

$$\frac{\hbar}{m_0} dt = \pm \frac{a_r a_o^2 \left(-\frac{r^2}{4a_o^2} + \frac{2r}{a_o} - 2\right)^{-1} \left(\frac{r}{a_o}\right)^{-2} e^{\frac{r}{a_o}}}{(a_r I_3(r) + b_r)^2 + 1} dr. \quad (81)$$

Integrating numerically Eq. (81), we plot the radial time equation (Fig.6) for this bound state. The electron moves between two radial extremities  $r = (4 - 2\sqrt{2})a_o$  and  $r = (4 + 2\sqrt{2})a_o$  constituting nodes for the different trajectories that the electron traces. At the nodes positions the radial velocity given by Eq. (81) vanishes.



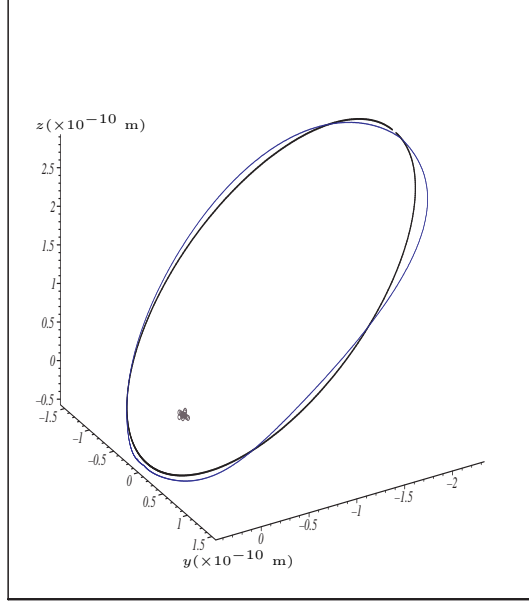


Fig8. This figure shows a comparison between the purely 3D classical trajectory to the one of the possible 3D quantum trajectories of the Hydrogen's electron for the state ( $E = -13.6/4$  eV,  $n = 2, l = 1, m_l = 1$ ). For the corresponding values of the hidden variables ( $a_r = 3.6$ ,  $b_r = 0.1$ ,  $a_\vartheta = 1, b_\vartheta = 0$ ,  $a_\varphi = 1, b_\varphi = 0$ ), we see easily from this picture, that the quantum trajectory can be considered as a deformation of the elliptic purely classical 3D trajectory. More comparison is done in Fig. 9, where projections of the two trajectories into  $YZ$  and  $XZ$  plans are done.

Taking Eqs. (78), (79) and (80) into Eqs. (55), (56) and (57), we get

$$\frac{\frac{4}{3} a_\varphi \sin^2(\vartheta)}{(a_\varphi \sin(\varphi) + b_\varphi \cos(\varphi))^2 + \cos^2(\varphi)} d\varphi = \pm \frac{a_r a_o^2 \left( -\frac{r^2}{4a_o^2} + \frac{2r}{a_o} - 2 \right)^{-1} \left( \frac{r}{a_o} \right)^{-2} r^{-2} e^{\frac{r}{a_o}}}{(a_r I_3(r) + b_r)^2 + 1} dr, \quad (82)$$

$$\frac{a_\varphi}{(a_\varphi \sin(\varphi) + b_\varphi \cos(\varphi))^2 + \cos^2(\varphi)} d\varphi = \pm \frac{a_\vartheta \left( \frac{8}{3} \sin^2(\vartheta) - 1 \right)^{-1} \sin^{-3}(\vartheta)}{\left[ a_\vartheta \left( \frac{\cos(\vartheta)}{\cos(2\vartheta) - 1} + \frac{1}{2} \log(|\tan(\frac{\vartheta}{2})|) \right) + b_\vartheta \right]^2 + 1} d\vartheta. \quad (83)$$

Integrating the last equations we plot the 3D quantum spatial trajectories (Fig.7). For this state, we find that the QTs are closed curves that are contained between the two extremities  $r = (4 - 2\sqrt{2}) a_o$  and  $r = (4 + 2\sqrt{2}) a_o$  constituting nodes. Note that, while the classical trajectory is an ellipse situated into an inclined plan (Figs.1), the QTs have complex forms and are not contained in a plan (Figs.7 and 8). Since the radial velocities vanish at the extremities, then, when the electron reaches the lowest extremity position  $r = r_{min} = (4 -$

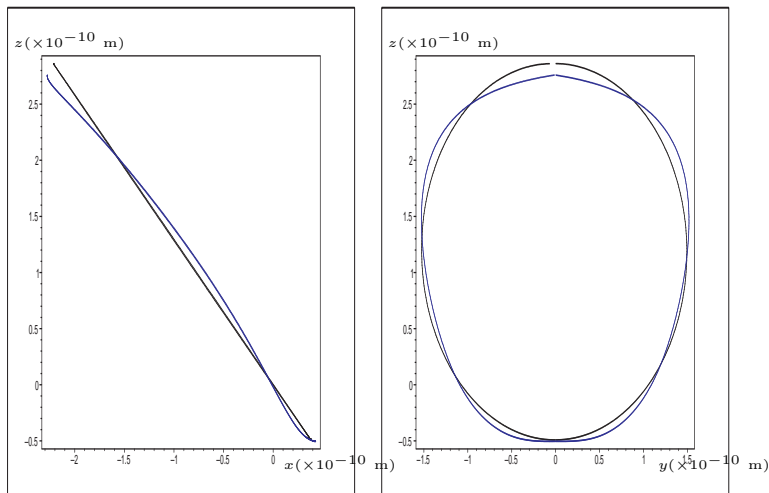


Fig9. Projection onto the  $XZ$  and  $YZ$  plans of the spatial trajectory for the state ( $E = -13.6/4$  eV,  $n = 2$ ,  $l = 1$ ,  $m_l = 1$ )( $a_r = 3.6$ ,  $b_r = 0.1$ ,  $a_\vartheta = 1$ ,  $b_\vartheta = 0$ ,  $a_\varphi = 1$ ,  $b_\varphi = 0$ ), and its corresponding purely classical trajectory. The quantum trajectory seems to be a deformation of the classical one.

$2\sqrt{2}a_o$  it must turn back to the highest extremity position  $r = r_{max} = (4 + 2\sqrt{2})a_o$  making the number of the trajectory cut branches two. The reason of this behavior is that the electron should turn around the nucleus making it trajectories to surround it.

Now, let us compare one specific QT integrated from Eqs. (82) and (83) with the corresponding classical trajectory plotted from the classical equations (48) and (50). Such comparison can be done only for the states for which  $m_l \neq 0$ , otherwise the classical conjugate momentum  $dM/d\varphi$  with respect to  $\varphi$  takes an imaginary value. This is the reason why we considered the state for which  $n = 2$ ,  $l = 1$  and  $m_l = 1$ . For this state, the corresponding constants  $\alpha$  and  $\beta$  take the values  $2\hbar^2$  and  $(\sqrt{3}/2)\hbar$  respectively. Fig.8 shows that for  $a_r = 3.6$ ,  $b_r = 0.1$ ,  $a_\vartheta = 1$ ,  $b_\vartheta = 0$ ,  $a_\varphi = 1$  and  $b_\varphi = 0$ , the QT goes approximately to the classical trajectory with an apparent residual deformation (Figs.8 and 9) that we assign to the residual quantum effects. To render this note more clear, we plotted in Fig.9 the projection of the two trajectories into  $XZ$  and  $YZ$  plans. The Fig.9 shows that the QT has a deformation of an ellipse.

It is useful to notice that for the different bound state studied above, the electron is trapped between two radial positions given by the two roots of the equation

$$E - V(r) - \frac{l(l+1)\hbar^2}{2m_0 r^2} = 0, \quad (84)$$

and, if the electron reaches an extremity position in the trapping zone delimited by the two roots, either it will return back on it way toward the other extremity or it will be pushed away from the trapping zone. We think that when the electron is pushed away from the trapping zone, it will either take a trajectory of another state (excited or fundamental) or it will be totally ejected from the atom. This fact is partially established in Fig.10 which shows that for the bound

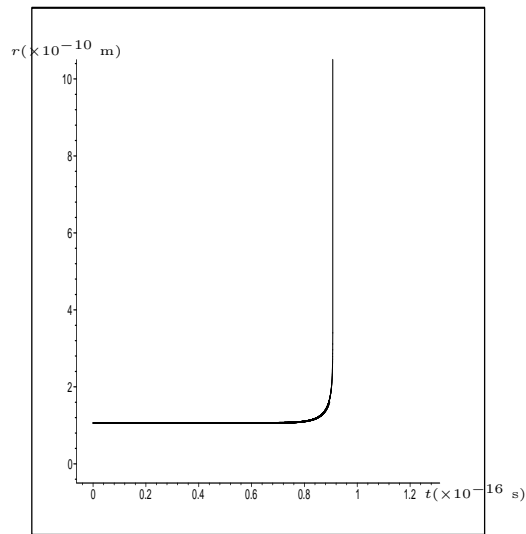


Fig10. The ejection of the electron from the atom when it leave the trapping zone ( $0 \leq r \leq 2 a_o$ ) in the case of the fundamental bound state ( $E = -13.6$  eV,  $n = 1$ ,  $l = 0$ ,  $m_l = 0$ ). We chose for the radial hidden variables the values  $a_r = 1.75$  and  $b_r = 0.5$ .

state ( $n = 1$ ,  $l = 0$ ,  $m_l = 0$ ), after crossing the position  $r = 2 a_0$ , which is the upper extremity of the trapping zone, the electron reaches in a limited time a position of about  $10^{10}$  m. This means that, after living the trapping zone the electron will be strongly ejected far from the atom and is no more bounded to it. That is in some disagreement with the standard quantum mechanics which suggests that for any position in the space, the atomic electron has a non vanishing probability to be bounded to the atom. A consequence of such a result is a partial localization of the electron in the space in the case of the bound states.

## 6- Conclusion

First, we emphasize that in this article we continued the work presented in Ref. [1] where we have established the 3D quantum law of motion that we apply in this paper to the central potential case and in particular to the Hydrogen's atom. We proceeded by three main steps, the first one is the establishment of the 3D-QSHJE and the quantum reduced action for the case of a central potential (Sec. 2). Then, in the second step, we established the 3D Quantum law of motion under the central potential (Sec. 3). Finally, in the third step, we plotted the 3D QTs of the Hydrogen's electron (Sec. 5). Analyzing the trajectories obtained in Sec. 5 for different bound states of the electron, we found three main outcomes.

The first outcome is the fact that for the bound state cases, the electron is trapped between two radial positions given by the two roots of the Eq.(84). A consequence of such a result is a partial localization of the electron in the space in the case of the bound states contradicting the standard quantum mechanics outcome which stipulates that for a giving bound state, the electron is localized in all the space.

The second outcome is the existence of nodes from which all the possible QTs plotted for the same state pass. In general, the positions of these nodes correspond to the zeros of the functions  $\mathcal{X}^{(nl)}$  and to the points where the radial velocity  $\dot{r}$  vanishes.

The third outcome concerns the fact that the QTs goes approximately to its corresponding purely classical trajectory for well chosen values the hidden variables. That reinforce the fact that the quantum equations of motion reduce to the classical ones.

## REFERENCES

1. T. Djama, Phys. Scr. 76 (2007) 82-92.
2. A. Bouda and T. Djama, Phys. Scr. 66 (2002) 97-104.
3. T. Djama, Phys. Scr. 75 (2007) 71-76.
4. C. Cohen-Tannoudji, B. Diu et F. Laloë, Mécanique quantique (Hermann, 1977), tome 1.
5. T. Djama, submitted to Found. Phys.
6. A. Nikiforov et V. Ouvarov, Fonctions spéciales de la physique mathématique (Mir, 1983).
7. A. E. Faraggi and M. Matone, *Int. J. Mod. Phys. A* 15, 1869.
8. E. R. Floyd, Phys. Lett. A 214, 259 (1996).